Agricultural Engineering Research Journal 5(3): 33-41, 2015
ISSN 2218-3906

DOI: 10.5829/idosi.aerj.2015.33.41

Modeling of Soil Pressure-Sinkage Behavior Using the Finite Element Method

[1]Majid Rashidi, [2]Reza Attarnejad, [3]Ahmmad Tabatabaeefar and [3]Alireza Keyhani

[1]Agricultural Engineering Research Department, Tehran Agricultural
and Natural Resources Research Center, AREEO, Varamin, Iran
[2]Civil Engineering Department, Faculty of Engineering, University of Tehran
[3]Power and Machinery Department, Faculty of Agricultural Biosystem Engineering, University of Tehran

Abstract: The finite element method (FEM) is a useful tool in the development of model for soil pressure-sinkage behavior and can be used to investigate and analyze the soil compaction. For this purpose, the finite element method was used to model soil pressure-sinkage behavior and a two-dimensional finite element model was developed to perform required numerical calculation. This program was written in FORTRAN. The soil material was considered as an elastoplastic material and the Drucker-Prager elastoplastic material model was adopted with the flow rule of associated plasticity. In order to deal with material non-linearity, incremental method was adopted to gradually load the soil and a total Lagrangian formulation was used to allow for the geometric non-linear behavior of soil. The FEM model was verified against previously developed models for one circular footing problem and one strip footing problem and the finite element program was used to predict the pressure-sinkage behavior of soil under footings. The statistical results of the study confirmed the validity of the FEM model and demonstrated the potential use of the FEM in prediction of soil pressure-sinkage behavior.

Key words: Finite element method · Pressure-sinkage · Drucker-prager · Elastoplastic · Soil compaction

INTRODUCTION

Agronomists are concerned about the effects of heavy tractors and agricultural machines on agricultural soils due to the possibly of excessive soil compaction that impedes root growth and hence reduces crop yields [1]. Soil compaction under tractors and farm machinery is of special concern because the weight of these machines has been increased dramatically in the last few years [2] and these implements create persistent subsoil compaction [3]. One of the most important causes of soil compaction is the soil response to pressure and sinkage imposed by wheels and tracks [2]. Therefore, the prediction of soil sinkage under loads is very important for determining the level of compaction in the soil. Furthermore, the ability to predict soil sinkage can enable agricultural engineers to till or traffic the soil when it is not in a highly compatible state or to estimate the damage being done to the soil structure due to their excessive loading when tillage or traffic is necessary [4].

Most studies dealing with soil sinkage have been experimental. One disadvantage of the experimental procedure is that it is laborious, time consuming and expensive. An alternative approach is to develop a numerical technique that can predict soil pressure-sinkage behavior. One such technique that can be used to predict soil sinkage is the finite element method (FEM). The FEM is now firmly accepted as a most powerful general technique for the numerical solution of a variety of problems encountered in engineering. Applications range from the stress analysis of solids to the solution of acoustical, neutron physics and fluid mechanics problems. Indeed the FEM is now established as a general numerical method for the solution of problems subjected to known boundary and/or initial value conditions. The basic concept of the FEM is the idealization of the continuum as an assemblage of a finite number of elements or small segments interconnected at nodal points. The behavior of the continuum when loaded is then predicted by approximating the behavior of the

Corresponding Author: Dr. Majid Rashidi, Ph.D., Agricultural Engineering Research Department,
Tehran Agricultural and Natural Resources Research Center, AREEO, Varamin, Iran.
E-mails: majidrashidi81@yahoo.com & m-rashidi@areeo.ac.ir.

elements. A solution of this set of equations constitutes a solution of the finite element system. For almost last 35 years this method has been touted as a powerful way to solve soil mechanics problems [2, 4-11].

Furthermore, the FEM offers significant promise for modeling of soil pressure-sinkage behavior. This method can accurately model complex loading geometries (tires, tracks, etc.) and the analysis can be performed easily on microcomputers. However, additional work is required to refine the FEM before it can be used to accurately predict soil behavior. These problems stem from the complex nature of agricultural soils. Agricultural soil experiences much greater strain than other materials (steel, concrete, etc.) that have typically been modeled by civil and mechanical engineers using the FEM. The nonlinear nature of agricultural soils is also a complicating factor because it does not obey linear elastic theory and it exhibits elastoplastic behavior [8]. Recent advances in development of constitutive relationship and theory of plasticity can make the FEM a more successful technique for modeling soil behaviors. Therefore, the overall objective of this study was to develop a numerical procedure to predict the soil sinkage. The specific objectives of the study were to develop a finite element program capable of predicting soil pressure-sinkage behavior and to verify the nonlinear finite element model by comparing its results with those of the verified finite element models.

MATERIALS AND METHODS

Material Model Development: Two sources of non-linearity are to be expected when a soil is under external loads, namely material and geometrical non-linearity [2, 10, 12]. Material non-linearity can be fully described by the stress-strain relationship. For an elastoplastic material behavior the incremental stress tensor can be related to the incremental strain tensor as [10]:

$$d\sigma_{ij} = C^{ep}_{ijkl} d\varepsilon_{kl} \tag{1}$$

where:

C^{ep}_{ijkl} = Elastoplastic constitutive matrix

$d\sigma_{ij}$ = Incremental stress tensor

$d\varepsilon_{kl}$ = Incremental strain tensor which is the summation of the incremental elastic strain tensor and incremental plastic strain tensor as [13]:

$$d\varepsilon_{ij} = d\varepsilon^{e}_{ij} + d\varepsilon^{p}_{ij} \tag{2}$$

The incremental elastic strain tensor $d\varepsilon^{e}_{ij}$ can be expressed by Hooke's law as [9]:

$$d\varepsilon^{e}_{ij} = \frac{(1+\upsilon)}{E} d\sigma_{ij} - \frac{\upsilon}{E} d\sigma_{kk}\delta_{ij} \tag{3}$$

where:

υ = Poisson's ratio

E = Modulus of elasticity

$d\sigma_{kk}$ = Incremental volumetric stress tensor

δ_{ij} = Kronecker delta

The incremental plastic strain tensor $d\varepsilon^{p}_{ij}$ can be expressed by the classical theory of plasticity as [9, 10]:

$$d\varepsilon^{p}_{ij} = d\lambda \frac{\partial F}{\partial \sigma_{ij}} \tag{4}$$

where:

$d\lambda$ = Plastic multiplier

F = Yield function

The incremental plastic strain tensor is actually a vector perpendicular to the tangent of the yield surface. This definition of the plastic strain is usually designated as associated plasticity [10].

The yield function of the Drucker-Prager for an elastoplastic material can be expressed as [9, 10]:

$$F = aJ_1 + J^{1/2}_{2D} - k = 0 \tag{5}$$

where:

J_1 = The first invariant of the stress tensor

J_{2D} = The second invariant of the deviatoric stress tensor

a,k = Soil parameters which can be defined as:

$$a = \frac{2\sin\varphi}{\sqrt{3}(3-\sin\varphi)} \tag{6}$$

$$k = \frac{6c\cos\varphi}{\sqrt{3}(3-\sin\varphi)} \tag{7}$$

where:

c = soil cohesion

φ = angle of soil internal friction

From equation 5 it can be concluded that the Drucker-Prager yield criterion accounts for both volumetric and shear behavior.

Finite Element Model Development: The governing equations of the finite element method (FEM) can be obtained by using the principle of virtual work. Consider the solid, in which the internal stresses σ, the distributed loads/unit volume *b* and external applied forces *f* form an equilibrium field, to undergo an arbitrary virtual displacement pattern δd^* which result in compatible strains $\delta\varepsilon^*$ and internal displacement δu^*. Then the principle of virtual work requires that [14]:

$$\int_{\Omega}(\delta\varepsilon^{*T}\sigma - \delta u^{*T}b)d\Omega - \delta d^{*T}f = 0 \tag{8}$$

where:
Ω = the domain of interest

Then the normal finite element discretising procedure leads to the following expressions for the displacement and strains within any element [13]:

$$\delta u^* = N\delta d^* \tag{9}$$

$$\delta\varepsilon^* = B\delta d^* \tag{10}$$

where:
N = Matrix of the shape function
B = Sum of the geometric linear and geometric non-linear strain-displacement matrix

Then the element assembly process gives:

$$\int_{\Omega}\delta d^{*T}(B^T\sigma - N^Tb)d\Omega - \delta d^{*T}f = 0 \tag{11}$$

where, the volume integration over the solid is the sum of the individual element contributions. Since this expression must be true for any arbitrary δd^* value:

$$\int_{\Omega}B^T\sigma d\Omega - f - \int_{\Omega}N^Tbd\Omega = 0 \tag{12}$$

For solution of nonlinear problems, equation 12 will not generally be satisfied at any stage of the computation and:

$$\psi = \int_{\Omega}B^T\sigma d\Omega - (f + \int_{\Omega}N^Tbd\Omega) \neq 0 \tag{13}$$

where:
ψ = the residual force vector

For an elastoplastic situation the material stiffness is continually varying and instantaneously the incremental stress-strain relationship is given by equation 1. For purpose of evaluating the element tangential stiffness matrix at any stage, the incremental form of the equation 13 must be employed. Thus, within an increment of load we have:

$$\Delta\psi = \int_{\Omega}B^T\Delta\sigma d\Omega - (\Delta f + \int_{\Omega}N^T\Delta bd\Omega) \tag{14}$$

Substituting for $\Delta\sigma$ from equation 1 result in:

$$\Delta\psi = K_T d - (\Delta f + \int_{\Omega}N^T\Delta bd\Omega) \tag{15}$$

where:
K_T = Element stiffness matrix associated with the geometric linear and geometric non-linear strain-displacement matrix and can be expressed as:

$$K_T = \int_{\Omega}B^TC_{ep}Bd\Omega \tag{16}$$

Finite Element Program Development: A plane-stress, plane-strain and axisymmetric finite element program [14] was modified and a finite element program, entitled PRESSINK, was developed using all the techniques, models, equations and assumptions previously discussed to take into account the material and geometrical non-linearity of soil. This program was written in FORTRAN for use on a personal computer and additional required subroutines were formulated and assembled to form a working program for two-dimensional elastoplastic geometrically non-linear analysis of plane-stress, plane-strain and axisymmetric problems. A modular approach was adopted for the program, in that separate subroutines were employed to perform the various operations required in non-linear finite element analysis. In order to deal with material non-linearity and obtain stress and strain information at different steps of a loading process, incremental method was adopted in this study. In addition, soil usually undergoes large deformation and strain and as we know the stiffness matrix of an element is dependent upon its geometric position and the equilibrium equations must be described by the geometric position after deformation [13]. To model the geometric non-linear behavior by the FEM, a total Lagrangian formulation was used in the program. The modification of the strain-displacement matrix and the evaluation of the strains using a deformation jacobian matrix were the main changes required to account for geometrically non-linear

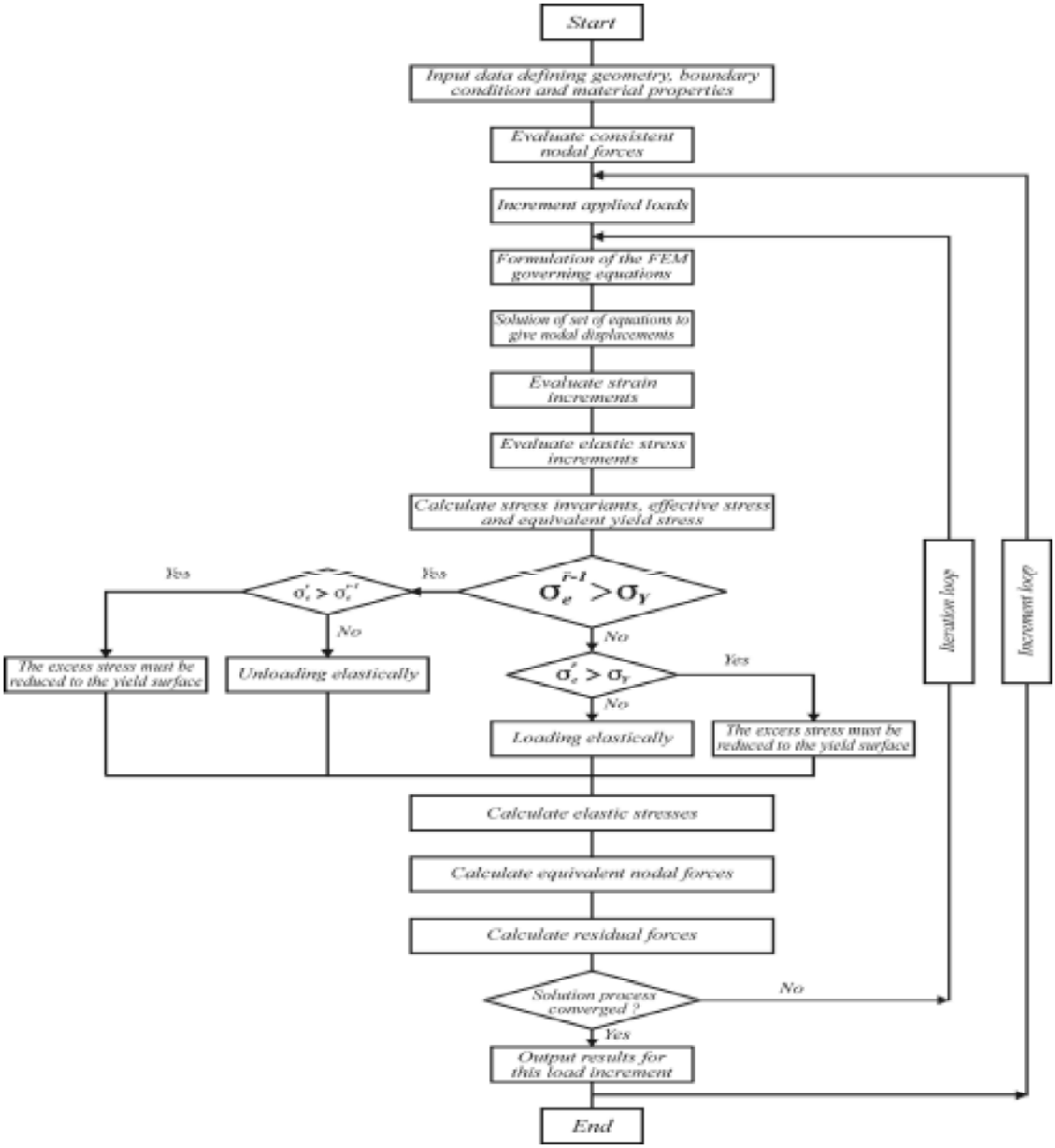

Fig. 1: Flow chart of the non-linear finite element analysis program

effects. The flow chart of the program is self-explanatory and is presented in Fig. 1 without further comments. In this flow chart:

σ_e^{r-1} = Effective stress in the $(r-1)^{th}$ iteration of non-linear solution

σ_e^{r} = Effective stress in the $(r)^{th}$ iteration of non-linear solution

σ_Y = Equivalent yield stress

Finite Element Model Verification: Footing problems are one of the most common verification techniques used in engineering application [4]. Because the intent of the study was to evaluate the potential use of the finite element method for prediction of soil pressure-sinkage behavior, it was decided that this goal could be met with published data.

Verification of the FEM Model using a Circular Footing Problem: Zienkiewicz and Humpheson [15] have given an

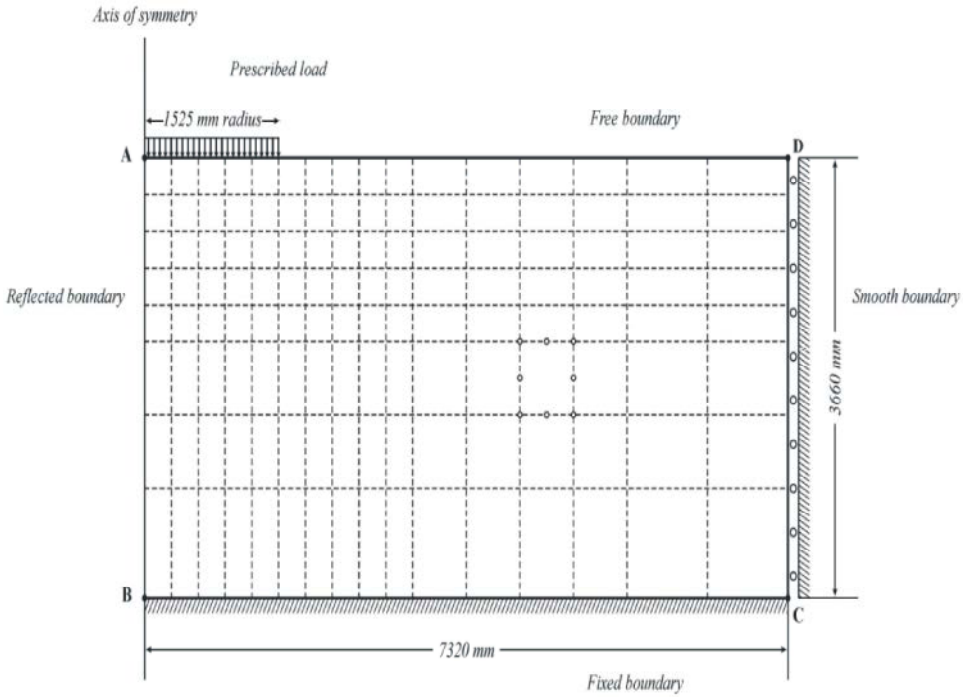

Fig. 2: Two-dimensional finite element mesh of the soil-circular footing system

Table 1: Soil parameters used for the finite element analysis of the soil-circular footing system

Parameter	Symbol	Value
Young's Modulus (MPa)	E	207
Poisson's ratio (no dimensional)	υ	0.30
Cohesion (kPa)	c	59.0
Angle of Internal Friction (deg)	φ	20.0

application of the finite element method for the analysis of pressure-sinkage behavior of soil beneath a circular footing. They used a two-dimensional finite element procedure in their investigation. Details of their investigation are given in Zienkiewicz and Humpheson [15] and only representative results are presented here.

Our finite element model was firstly verified by using this circular footing problem. In order to verify the finite element model, a two-dimensional FEM mesh was generated within a rectangular 7.32 m long and 3.66 m wide. The FEM mesh that was used to model the axisymmetric geometry of the soil-circular footing system in two-dimensional view is shown in Fig. 2. The total number of nodal points and elements were 433 and 128, respectively. The eight-node serendipity quadrilateral elements were used to represent the soil material. These elements were chosen as it was claimed that they give a more accurate answer for larger mesh sizes and also they uses numerical integration to determine their volume and surface area. These elements are easily numerically integrated by using Gauss-Legendre rule [16, 17]. For the elements used in this study, Hinton and Owen [16] advised using 2-point integration, even though our program allowed 2- or 3-point integration. Since the problem was symmetric about the vertical axis AB, only one half of the system was meshed and considered during the analysis. From Fig. 2 it can be seen that the left-side boundary line AB was considered as a reflected boundary and the nodes on the bottom boundary line BC were constrained in both horizontal and vertical direction. The nodes on the right-side boundary line CD were constrained in horizontal direction, whilst the nodes on the top boundary line AD were free of any constrains. The circular footing was assumed to be a rigid body and the loading was distributed evenly over the centermost five elements at the top of the finite element mesh. Soil parameters used for the non-linear finite element analysis of the soil-circular footing system adopted from Zienkiewicz and Humpheson [15] are shown in Table 1. For the finite element analysis, appropriate boundary conditions information, material properties and nodal and elemental data were input as required. The load application on the finite element model was simulated in an incremental manner and the total load of 1400 kPa was applied monotonically in increments of 280 kPa each.

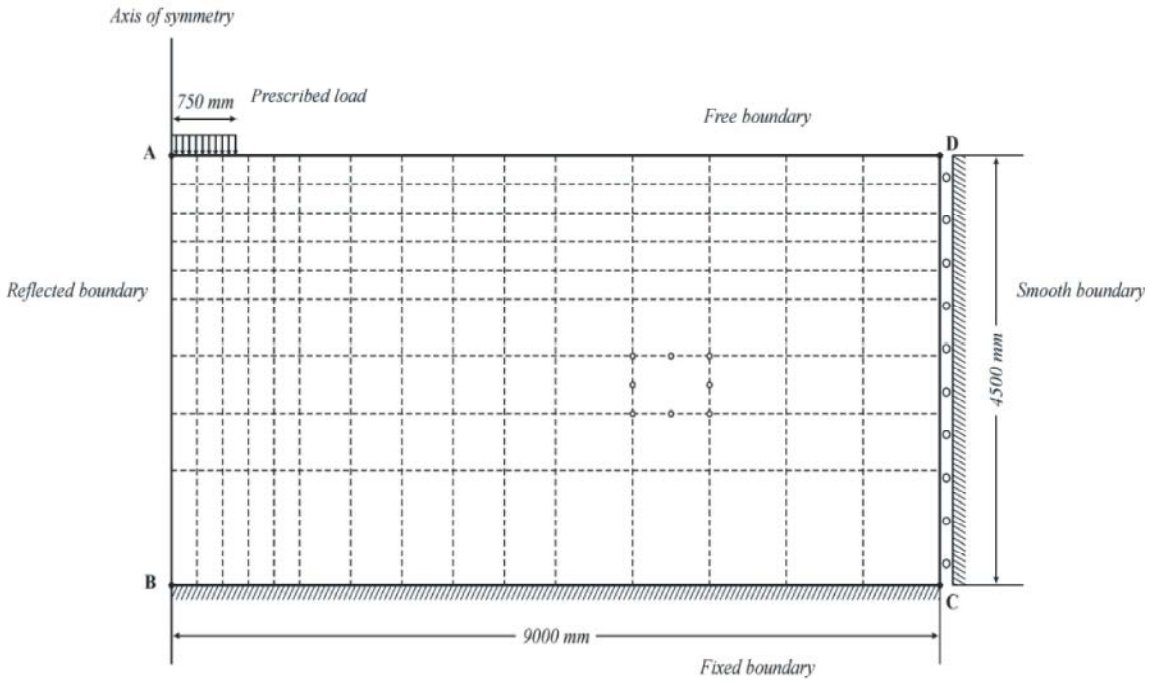

Fig. 3: Two-dimensional finite element mesh of the soil-strip footing system

Table 2: Soil parameters used for the finite element analysis of the soil-strip footing system

Parameter	Symbol	Value
Young's Modulus (MPa)	E	69.0
Poisson's ratio (no dimensional)	υ	0.30
Cohesion (kPa)	c	103.5
Angle of Internal Friction (deg)	φ	20.0

Verification of the FEM Model using a Strip Footing Problem: Siriwardane and Desai [18] have given another application of the finite element method for the analysis of pressure-sinkage behavior of soil beneath a strip footing. They used a three-dimensional finite element procedure in their investigation. Details of their investigation are given in Siriwardane and Desai [18] and only representative results are presented here.

Our finite element model was further verified by using this strip footing problem. As before, in order to verify the finite element model, a two-dimensional FEM mesh was generated within a rectangular 9.0 m long and 4.5 m wide. Fig. 3 shows the FEM mesh that was used to model the plane-strain geometry of the soil-strip footing system in two-dimensional view. The total number of nodal points and elements were 454 and 135, respectively. In this problem, the eight-node serendipity quadrilateral elements were used to represent the soil material and the Gauss-Legendre 2-point integration rule was used to determine their volume and surface. Since the problem was symmetric about the vertical axis AB, only one half of the system was meshed and considered during the analysis. From Fig. 3 it can be seen that the left-side boundary line AB was considered as a reflected boundary and the nodes on the bottom boundary line BC were constrained in both horizontal and vertical direction. The nodes on the right-side boundary line CD were constrained in horizontal direction and the nodes on the top boundary line AD were free of any constrains. The strip footing was assumed to be a rigid body and the loading was distributed evenly over the left-side three elements at the top of the finite element mesh. Soil parameters used for the non-linear finite element analysis of soil-strip footing system adopted from Siriwardane and Desai [18] are shown in Table 2. For the finite element analysis, appropriate boundary conditions information, material properties and nodal and elemental data were input as required. The load application on the finite element model was simulated in an incremental manner and the total load of 1900 kPa was applied monotonically in increments of 380 kPa each.

RESULTS AND DISCUSSION

Results of the finite element analyses included information on displacement of each nodal point. For each

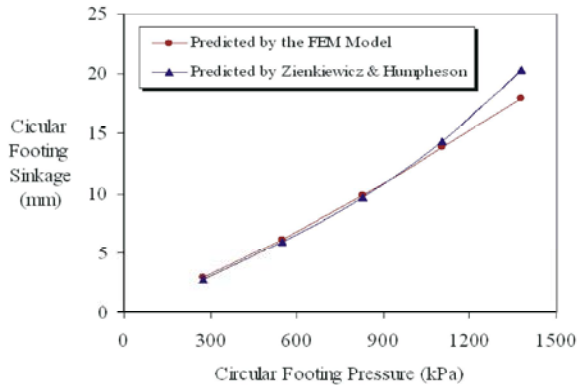

Fig. 4: Pressure-sinkage curve of the circular footing predicted using the FEM model in compared with that predicted previously by Zienkiewicz and Humpheson [15]

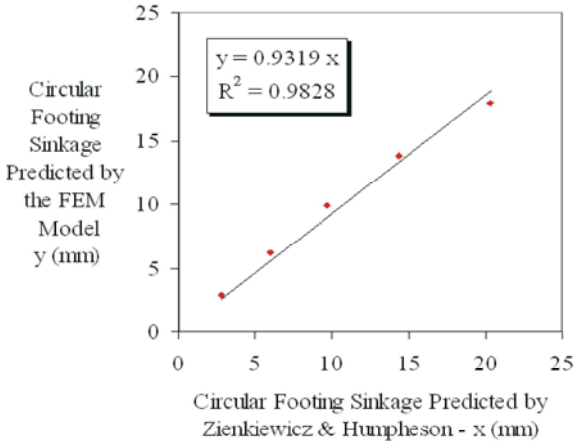

Fig. 5: Circular footing sinkage values predicted using the FEM model and circular footing sinkage values predicted previously by Zienkiewicz and Humpheson [15] are plotted against each other and fitted with a linear equation with zero intercept

incremental load, the displacement of each nodal point was computed. This process was continued until the total load amount was applied. At this point, the incremental loading was stopped to complete the simulation of soil pressure-sinkage behavior.

Results of the FEM Analysis for the Circular Footing Problem: Fig. 4 shows the predicted soil pressure-sinkage curve at the center of the footing surface, which was developed from the results of the finite element analysis. A maximum soil sinkage value was predicted at the footing surface beneath the central axis of the circular footing for all load increments and additional loadings yielded larger increments in soil sinkage. These large values clearly showed that large strain theory could not be used without the incremental loading approach. Fig. 4 also shows the predicted soil pressure-sinkage curve at the center of the footing surface, which was developed from the results obtained previously by Zienkiewicz and Humpheson [15]. From comparison of two curves, it could be concluded that both the analyses gave almost similar results. A linear regression was performed to verify the validity of the FEM model. Fig. 5 shows that the circular footing sinkage values predicted using the FEM model and those predicted previously by Zienkiewicz and Humpheson [15] were plotted against each other and fitted with a linear equation with zero intercept. The slope of the line of best fit and its coefficient of determination were 0.93 and 0.98, respectively. Root of mean squared errors (RMSE) and mean relative percentage deviation (MRPD) were used to check the discrepancies between the predicted results using the FEM model and those predicted previously by Zienkiewicz and Humpheson [15]. The amounts of RMSE and MRPD were 1.10 mm and 5 % respectively and regarding the statistical results, the validity of the FEM model was confirmed. More likely reason for such negligible discrepancies between the predicted results using the non-linear geometric and material FEM model and those predicted previously by Zienkiewicz and Humpheson [15] probably stem from the fact that for this problem, the deformations in the soil are governed predominantly by the material non-linearity rather than by geometric and material non-linearity.

Results of the FEM Analysis for the Strip Footing Problem: Fig. 6 shows the predicted soil pressure-sinkage curve at the axis of symmetry of the footing surface that was developed from the results of the FEM analysis. Again, a maximum soil sinkage value was predicted at the footing surface beneath the axis of symmetry of the strip footing for all load increments and additional loadings yielded larger increments in soil sinkage. These large values again confirmed using of large strain theory in conjunction with the incremental loading approach. Fig. 6 also shows the soil pressure-sinkage curve at the axis of symmetry of the footing surface that was developed from the results obtained previously by Siriwardane and Desai [18]. From comparison of two curves, it could be concluded that both analyses generally represent similar curves, but the sinkage values predicted by the FEM model are relatively greater than

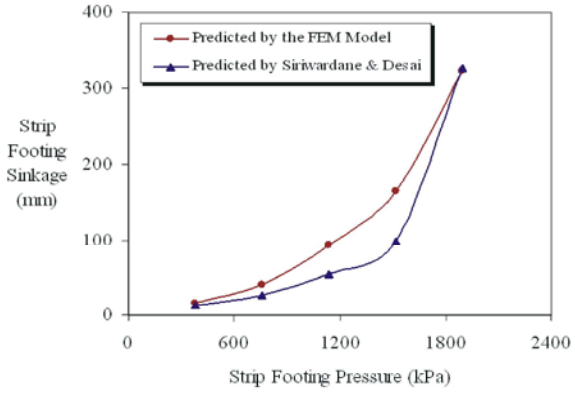

Fig. 6: Pressure-sinkage curve of the strip footing predicted using the FEM model in compared with that predicted previously by Siriwardane and Desai [18]

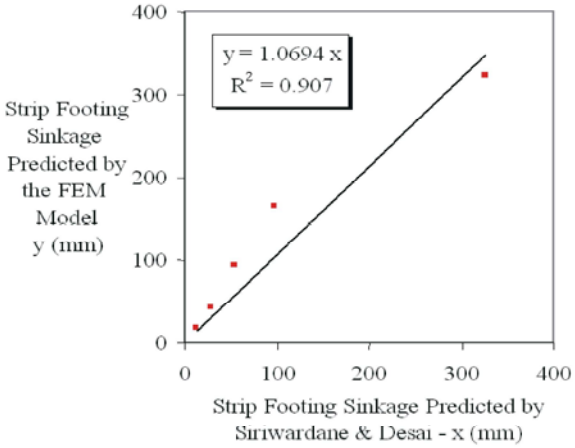

Fig. 7: Strip footing sinkage values predicted using the FEM model and strip footing sinkage values predicted previously by Siriwardane and Desai [18] are plotted against each other and fitted with a linear equation with zero intercept

those predicted previously by Siriwardane and Desai [18]. As before, a linear regression was performed to verify the validity of the FEM model. Fig. 7 shows that the strip footing sinkage values predicted using the FEM model and those predicted previously by Siriwardane and Desai [18] were plotted against each other and fitted with a linear equation with zero intercept. The slope of the line of best fit and its coefficient of determination were 1.07 and 0.91, respectively. Again, root of mean squared errors (RMSE) and mean relative percentage deviation (MRPD) were used to check the discrepancies between the predicted results using the FEM model and those predicted previously by Siriwardane and Desai [18]. The amounts of RMSE and MRPD were 35.0 mm and 27 % respectively. More likely reason for such discrepancies between the predicted results using the non-linear geometric and material FEM model and those predicted previously by Siriwardane and Desai [18] probably stem from our modeling due to the geometrically nonlinear assumption and can be due to the fact that for this problem, the soil deformations are governed by material and geometrical non-linearity and to reasonably predict soil pressure-sinkage behavior in soil problems, both material and geometrical non-linearity should be account over the entire soil volume being modeled.

CONCLUSIONS

Results of the study confirmed the validity of the new FEM model and demonstrated the potential use of the FEM in predicting soil pressure-sinkage behavior. However, experimental verification of the model is necessary before the model can be recommended for wider use. Anyway, the FEM analysis of soil pressure-sinkage behavior has led to these conclusions:

- Firstly, the FEM proved to be a good tool for predicting soil pressure-sinkage behavior too.
- Secondly, to reasonably predict soil pressure-sinkage behavior using the FEM models, both material and geometrical non-linearity should be account for the entire soil volume being modeled.

REFERENCES

1. Al-Adawi, S.S. and R.C. Reeder, 1996. Compaction and subsoiling effects on corn and soybean yields and soil physical properties. Trans. ASAE, 39: 1641-1649.
2. Abu-Hamdeh, N.H. and R.C. Reeder, 2003. Measuring and predicting stress distribution under tractive devices in undisturbed soil. Biosys. Eng., 85: 493-502.
3. Çakir, E., E. Gülsoylu and G. Keçecioðlu, 1999. Multiplate penetration tests to determine soil stiffness moduli of ege region. In Proceedings of International Congress on Agricultural Mechanization and Energy, 26-27 May 1999, Adana-Turkey, pp: 103-107.
4. Raper, R.L. and D.C. Erbach, 1990a. Effect of variable linear elastic parameters on finite element prediction of soil compaction. Trans. ASAE, 33: 731-736.
5. Girijavallabhan, A.M. and L.C. Reese, 1968. Finite element method for problems in soil mechanics. J. Soil Mech. Found. Div., Proc. ASCE, 94: 473-496.

6. Perumpral, J.V., J.B. Liljedahl and W.H. Perloff, 1971. The finite element method for predicting stress distribution and soil deformation under a tractive device. Trans. ASAE, 14: 1184-1188.
7. Pollock, D., J.V. Perumpral and T. Kuppusamy, 1985. Finite element analysis of multipass effects of vehicles on soil compaction. Trans. ASAE, 29: 45-50.
8. Raper, R.L. and D.C. Erbach, 1990b. Prediction of soil stresses using the finite element method. Trans. ASAE, 33: 725-730.
9. Arya, K. and R. Gao, 1995. A non-linear three-dimensional finite element analysis of subsoiler cutting with pressurized air injection. J. Agri. Eng. Res., 61: 115-128.
10. Mouazen, A.M. and M. Nemenyi, 1999. Finite element analysis of subsoiler cutting in non-homogeneous sandy loam soil. Soil Till. Res., 51: 1-15.
11. Defossez, P. and G. Richard, 2002. Models of soil compaction due to traffic and their evaluation. Soil Till. Res., 67: 41-64.
12. Naylor, D.J. and G.N. Pande, 1981. Finite Elements in Geotechnical Engineering. Swansea, U.K.: Pineridge Press Limited.
13. Shen, J. and R.L. Kushwaha, 1998. Soil-Machine Interaction, A Finite Element Perspective. New York: Marcel Dekker, Inc.
14. Owen, D.R.J. and E. Hinton, 1980. Finite Elements in Plasticity. Swansea, U.K.: Pineridge Press Limited.
15. Zienkiewicz, O.C. and C. Humpheson, 1977. Viscoplasticity: a generalized model for description of soil behavior. In: Numerical Methods in Geotechnical Engineering. (Desai, C.S. and J.T. Christian eds.), McGraw-Hill Book Company, New York, NY.
16. Hinton, E. and D.R.J. Owen, 1979. An Introduction to Finite Element Computation. Swansea, U.K.: Pineridge Press Limited.
17. Bathe, K.J., 1996. Finite Element Procedures in Engineering Analysis. Englewood Cliffs, New Jersey: Prentice-Hall, Inc.
18. Siriwardane, H.J. and C.S. Desai, 1983. Computational procedures for nonlinear three-dimensional analysis with some advanced constitutive laws. Int. J. Numer. Anal. Method. Geomech., 7: 143-171.